

HOSTED BY



Contents lists available at ScienceDirect

# Atmospheric Pollution Research

journal homepage: <http://www.journals.elsevier.com/locate/apr>

## Classification and chemical compositions of individual particles at an eastern marginal site of Tibetan Plateau

Jingsen Fan <sup>a, b</sup>, Longyi Shao <sup>a, \*</sup>, Ying Hu <sup>a</sup>, Jianying Wang <sup>a</sup>, Jing Wang <sup>a</sup>, Jianzhong Ma <sup>c</sup><sup>a</sup> State Key Laboratory of Coal Resources and Safe Mining, and School of Geoscience and Surveying Engineering, China University of Mining and Technology (Beijing), Beijing 100083, China<sup>b</sup> Collaborative Innovation Center of the Comprehensive Development and Utilization of Coal Resource, Hebei Province and The Resources Surveying and Researching Laboratory of HeBei Province, Hebei University of Engineering, Handan 056038, China<sup>c</sup> Chinese Academy of Meteorological Sciences, Beijing 100081, China

### ARTICLE INFO

#### Article history:

Received 8 December 2015

Received in revised form

13 April 2016

Accepted 21 April 2016

Available online 13 May 2016

#### Keywords:

Shangri-La

TEM-EDX

Mixing state

Individual particles

Tibetan Plateau

### ABSTRACT

Aerosol particles at Shangri-La, an eastern marginal site of Tibetan Plateau, were collected in July and August 2011. Morphologies and elemental compositions of individual particles were investigated through transmission electron microscopy coupled with energy dispersive X-ray spectroscopy. More than 14 elements were detected in the aerosol particles, and S were detected in more than 70% of the 292 analyzed particles. Six morphological types of individual particles were identified: soot, fly ash, complex secondary particles, crustal minerals, organic particles, and metal particles. The aerosol particles mainly comprised mineral particles (36.02%) and complex secondary particles (30.73%), followed by organic particles (17.38%), soot (8.06%), fly ash (6.08%), and metal particles (1.01%). The diameters of fly ash, soot, and metal particles were less than 2  $\mu\text{m}$ . Approximately 81% of the particles were internally or externally mixed with two or more aerosol components from different sources. Soot, fly ash, organic, and fine mineral particles were commonly internally mixed with S-rich particles. Mineral particles tended to commonly associate with visible coatings, probably formed through chemical reactions on the surface of the particles. Back-trajectories revealed that air mass arriving at Shangri-La were transported from Northeast Burma, a region of the Indian subcontinent.

Copyright © 2016 Turkish National Committee for Air Pollution Research and Control. Production and hosting by Elsevier B.V. This is an open access article under the CC BY-NC-ND license (<http://creativecommons.org/licenses/by-nc-nd/4.0/>).

### 1. Introduction

Atmospheric aerosols are gaining considerable attention because they are crucial in many climate and environmental processes (Buseck et al., 2000). Aerosol particles affect the climate directly by scattering and absorbing solar radiation and indirectly by regionally and globally altering cloud properties and precipitation (Griessbach et al., 2013; Rozanov et al., 2014). Thus, studying the physicochemical characteristics of atmospheric aerosols is essential in understanding the various phenomena that affect the behavior of aerosol particles in the atmosphere (Braziewicz et al., 2004). Understanding the chemical and physical properties of background aerosols facilitate their source determination, thus

elucidating the mechanism of the long-range transport of anthropogenic pollutants and validating both regional and global atmospheric models (Fattori et al., 2005; Toscano et al., 2005). In addition, the chemical compositions of aerosols from remote areas are a valuable reference for studying the rapid industrialization-driven evolution of the atmosphere.

The Shangri-La background station is located in the eastern margin of the Tibetan Plateau and the hinterlands of the Hengduan mountain range. The Tibetan Plateau, called the roof of the world, is the highest and most extensive plateau and has an area of  $2.5 \times 10^6 \text{ km}^2$  and a mean elevation of  $>4500 \text{ m}$ . In particular, the Tibetan Plateau plays a crucial role in the climatology of and atmospheric circulation in Asia and is regarded a sensitive region for global climate change owing to its special landform, ecosystem, and monsoon circulation (Qiu, 2008). Particularly in summers, as an elevated heat source, the low pressure over the Tibetan Plateau draws moist, warm air from the Indian Ocean to the continent, thus affecting summer monsoon circulation in Asia. The atmosphere of

\* Corresponding author. Tel.: +86 10 62339303.

E-mail address: [ShaoL@cumt.edu.cn](mailto:ShaoL@cumt.edu.cn) (L. Shao).

Peer review under responsibility of Turkish National Committee for Air Pollution Research and Control.

the area, particularly the aerosol compositions, has been extensively studied (Cong et al., 2010a; Huang et al., 2010; Ming et al., 2010; Wan et al., 2015; Zhao et al., 2013); the results indicate that its atmospheric environment is affected by long-range transported pollutants, such as heavy metals and black carbon. However, only few studies have focused on individual aerosol particles in the Tibetan Plateau (Cong et al., 2010b; Duo et al., 2015; Hu et al., 2013; Li et al., 2015; Zhang et al., 2001); studies on Shangri-La have focused mainly on gases (Fang et al., 2012; Gao et al., 2013; Ma et al., 2014) and visibility (Yang, 2013).

Transmission electron microscopy is a microscopy technique in which a beam of electrons is transmitted through an ultra-thin specimen, interacting with the specimen as it passes through it. Transmission electron microscopy coupled with energy dispersive X-ray spectroscopy (TEM-EDX) has been used to characterize individual particles and obtain detailed information on the morphologies, sizes, elemental compositions, and internal structures of individual aerosol particles. Studying the detailed analysis information of individual aerosol particles is crucial to evaluate their effects on climate and human health both locally and regionally (Lu et al., 2007; Shao et al., 2007). Individual particle optical properties depending on their aging properties or mixing states can be well revealed by laboratory and field measurements and theoretical calculations (Adachi and Buseck, 2010; Moffet and Prather, 2009; Thompson et al., 2012). Individual particle analysis can provide the mixing state of these non-refractory particles and explain heterogeneous reactions on particle surfaces during air pollution episodes (Adachi et al., 2014; Fu et al., 2012; Yang et al., 2012; Zhang et al., 2013). TEM is commonly used to study individual aerosol particles (Li et al., 2010a; Shi et al., 2012; Smith et al., 2012; Pósfai et al., 2013; Ueda et al., 2014; Li et al., 2016).

In this study, aerosol particles were collected at the Shangri-La regional atmosphere background station in Tibet during the summer of 2011, and the morphology and elemental compositions of individual aerosol particles were analyzed through TEM-EDX. The possible sources and heterogeneous reactions are discussed.

## 2. Materials and methods

### 2.1. Sampling

The Shangri-La regional atmosphere background station is located in the Diqing Tibetan Autonomous Prefecture (Elevation 3580 m; Lin et al., 2009). Here, June–October and November–May are the wet and dry seasons, respectively (Xie and Zhang, 2000). Shangri-La is located northwest of Yunnan Province of China, in the eastern margin of Qinghai-Tibet Plateau and the hinterlands of the Hengduan mountain range.

Aerosol particles were collected on copper TEM grids coated with a carbon film (300-mesh, China) using a KB-2F single-stage cascade impactor with a 0.5-mm-diameter jet nozzle at an air flow rate of 1 L/min. Theoretical collection efficiency calculations for the impactor are well established (Marple et al., 1993). The sampling time varied from 20 to 80 min depending on particle loading, which was estimated from the visibility (Li et al., 2011). The meteorological parameters during the sampling period were automatically recorded using Kestral 4000 (Table 1).

### 2.2. Experimental

TEM: Aerosol samples were analyzed using TEM-EDX at the China University of Petroleum. Samples were placed in an F20 FETEM (with an attached PV9000 spectrometer), and the spectral acquisition time was 30 s. The elemental composition of the samples was determined through EDX at 200 kV. Cu was excluded from

the analysis because the TEM grids were composed of Cu. The distribution of aerosol particles on the TEM grids was nonuniform; coarse particles were present near the center, and fine particles were present at the periphery. Therefore, to ensure that the analyzed particles were representative, particles from five areas from the center and periphery of the sampling spot on each grid (Li et al., 2013) were analyzed.

Back-trajectory calculation: The backward trajectories at Shangri-La from July 16, 2011, to August 01, 2011, were simulated using the Hybrid Single-Particle Lagrangian Integrated Trajectory (version 4.8) model. The endpoints were set at 100, 500, and 1000 m above the ground level. Global Data Assimilation System (GDAS) output dataset was used and the vertical motion method in the calculations is the default model selection.

## 3. Results

### 3.1. Nature of individual aerosol particles

The aerosol composition at the Shangri-La regional atmosphere background station was complex. More than 14 elements were detected through EDX (Fig. 1). S were detected in more than 70% of the 292 analyzed particles. K in more than 50%, and Ca, Mg, Fe, and Al in more than 25% of the 292 analyzed particles; P, Na, Cl, and heavy metals (e.g., Mn, Ti, and Zn) occurred in less than 20%.

Compared with the brown haze particles around Beijing, in which more than 18 elements were detected and S was present in more than 87% of the analyzed particles (Li and Shao, 2009a), the aerosol particles at Shangri-La were chemically less complex. However, the high frequency of S in the aerosol particles indicated that the particles were affected by human activities.

### 3.2. Individual particle types

Six types of individual particles, namely soot, fly ash, complex secondary particles, minerals, organic particles, and metal particles, were classified on the basis of their morphologies and elemental compositions (Table 2). “Element-rich” in the sub types means that the analyzed particles are mainly composed of this element occupies the first position in the chemical composition of the analyzed particles.

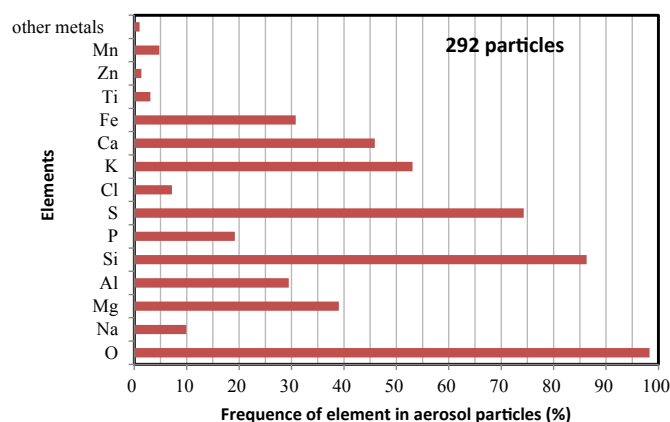
The morphology of soot particles exhibited individual chains and compact aggregates. The main component was C, which mainly originated from fossil fuel and biomass burning by local residents (Fig. 2a). One soot aggregate may contain ten to hundreds of C spheres, with typical diameters of 10–100 nm and a maximum of 150 nm. The high-resolution TEM image of soot spheres exhibited the discontinuous onion-like structure of a graphitic layer (Li and Shao, 2009a). Soot particles enhance the production of secondary species, such as sulfate and nitrate, on their surface (Wang et al., 2010).

Fly ash has a typical spherical morphology and is generally composed of Si and Al and occasionally contains minor quantities of Na, Mg, S, K, Ca, and Fe (Fig. 2b). They are typical anthropogenic aerosols that originate from coal combustion during heating and industrial activities. Such refractory particles with small sizes (diameter <1  $\mu\text{m}$ ) are usually mixed with secondary sulfate particles. The presence of fly ash particles at Shangri-La is attributable to long-distance transportation because no other major anthropogenic sources are in close proximity to the site; the nearest township is approximately 30 km from the station.

The composition of secondary particles is complex. Three types of secondary particles were identified, namely K-rich, S-rich, and  $\text{CaSO}_4$  particles. Ca-S, K-, and S-rich particles are often referred to as

**Table 1**  
Sampling information.

NO.	Date	T, °C	RH, average/%	P/hPa	Weather conditions	Cumulative time
E2	2011/07/17	18	55.9	658	Sunny	50 min
D4	2011/07/17	17.8	57	656	Sunny	40 min
Q3	2011/07/17	15.9	59	655.7	Sunny	20 min
J3	2011/07/22	19.2	49.8	655.9	Cloudy	30 min
E4	2011/07/29	22.5	47.9	656.5	Cloudy	30 min
R1	2011/07/18	14.2	70.8	658.9	Rainy	40 min
E1	2011/07/30	12.1	99.7	659	Rainy	20 min

**Fig. 1.** Frequencies of elements present in individual aerosol particles.

complex secondary particles in the atmosphere (Vester et al., 2007).

Most K-rich particles are irregularly shaped. K-rich particles also contain O and P (Fig. 2c). K-rich particles in haze mostly contain N, Na, O, S, and K and are free of Cl. In addition, diffraction patterns indicate the presence of  $K_2SO_4$  and  $KNO_3$ , which are easily damaged by a strong electron beam, implying that they are mixed with N-containing compounds (Li et al., 2010b). K-rich particles are abundant inorganic aerosol components of haze and serve as tracers for biomass burning (Adachi and Buseck, 2008; Li et al., 2010b; Niemi et al., 2006).

In addition to S, S-rich particles contain O in major quantities and K in minor quantities. A few of these particles were spherical (Fig. 2d). In addition, these particles were beam sensitive (Fig. 2e), leaving behind S-rich residues and one or more particles, such as

soot, fly ash, organic particles, fine-grained minerals, and metal particles. S-rich particles are major inorganic aerosol constituents of haze, and most are considered to be  $(NH_4)_2SO_4$  (Li et al., 2010b). The abundant  $(NH_4)_2SO_4$  particles in Beijing air are formed through chemical reactions between  $NH_3$  and  $H_2SO_4$  (Yao et al., 2003).

$CaSO_4$  particles are tiny, needle-like, and rectangular or amorphous and are mainly composed of O, S, and Ca (Fig. 2f). Most were aggregates of two or more rectangular particles.  $CaSO_4$  particles are sensitive to strong TEM electron beam. They were most probably formed through aqueous chemical reactions between calcite and  $H_2SO_4$  (Guo et al., 2010).

The element composition of mineral particles, which can be irregularly or regularly shaped, is generally complex. Mineral particles are stable to the electron beam. Crustal mineral particles contain dry and hygroscopic particles and individual or complex aggregates (Fig. 2g). They originate from dust or crust and are stable under a strong electron beam. A few mineral particles were encapsulated by visible coatings, which were mainly O, Ca (or Mg), S (minor), Cl, and N (N is inferred when no elements are detected in the amorphous film). The coatings are amorphous and sublime under a strong beam.

Organic aerosol particles tend to have irregular shapes, and their elemental compositions showed abundant C and minor quantities of O, S, K, and P. Organic particles were stable under a strong electron beam (Fig. 2h). Shangri-La is rich in forest resources and thus had abundant organic aerosol particles. Tar ball is a regular sphere with a smooth surface and is primarily composed of C. Tar ball particles were stable under a strong electron beam (Fig. 2i). The tar balls were larger than the soot particles and lacked graphitic structures (Pósfai and Buseck, 2010). In addition, their organic compositions resembled those of atmospheric humic-like substances (Tivanski et al., 2007). Tar ball particles are considered to originate from biomass burning (Chakrabarty et al., 2006; Pósfai et al., 2004).

**Table 2**  
Types of individual aerosol particles.

Particle types	Particle sub-types	Elemental characteristics	Physical characteristics	Source
Soot	Soot	Mainly C	Individual chain and chain aggregates	Coal burning, vehicle exhaust and biomass burning
Fly ash	Fly ash	Mainly Al, Si, sometimes Ca, Fe,	Regular rounded shape	Coal burning
Complex secondary particles	K-rich	K-rich	Easily damaged by strong electron beam	Crust, secondary reaction in industry and atmosphere, dust
	S-rich	S-rich, O, S, minor Cu	Rounded shape, extremely beam sensitive, then become the foamy	
Mineral particles	Ca-S	$CaSO_4$	Strip or drusy	Dust, crust
	Crustal mineral	Mainly Si, Al	Dry and hygroscopic particles, individual or complex aggregates, irregular	
Organic particles	Organic	Mainly C	Organic monomer or internally mixed with other particles, stable in strong electron beam	Plant and secondary reaction
	Tar ball	Mainly C	Regular rounded shape, smooth surface, stable in strong electron beam	Biomass and biofuel burning
Metal particles	Metal	Fe or Zn	Spherical or irregular	Industry

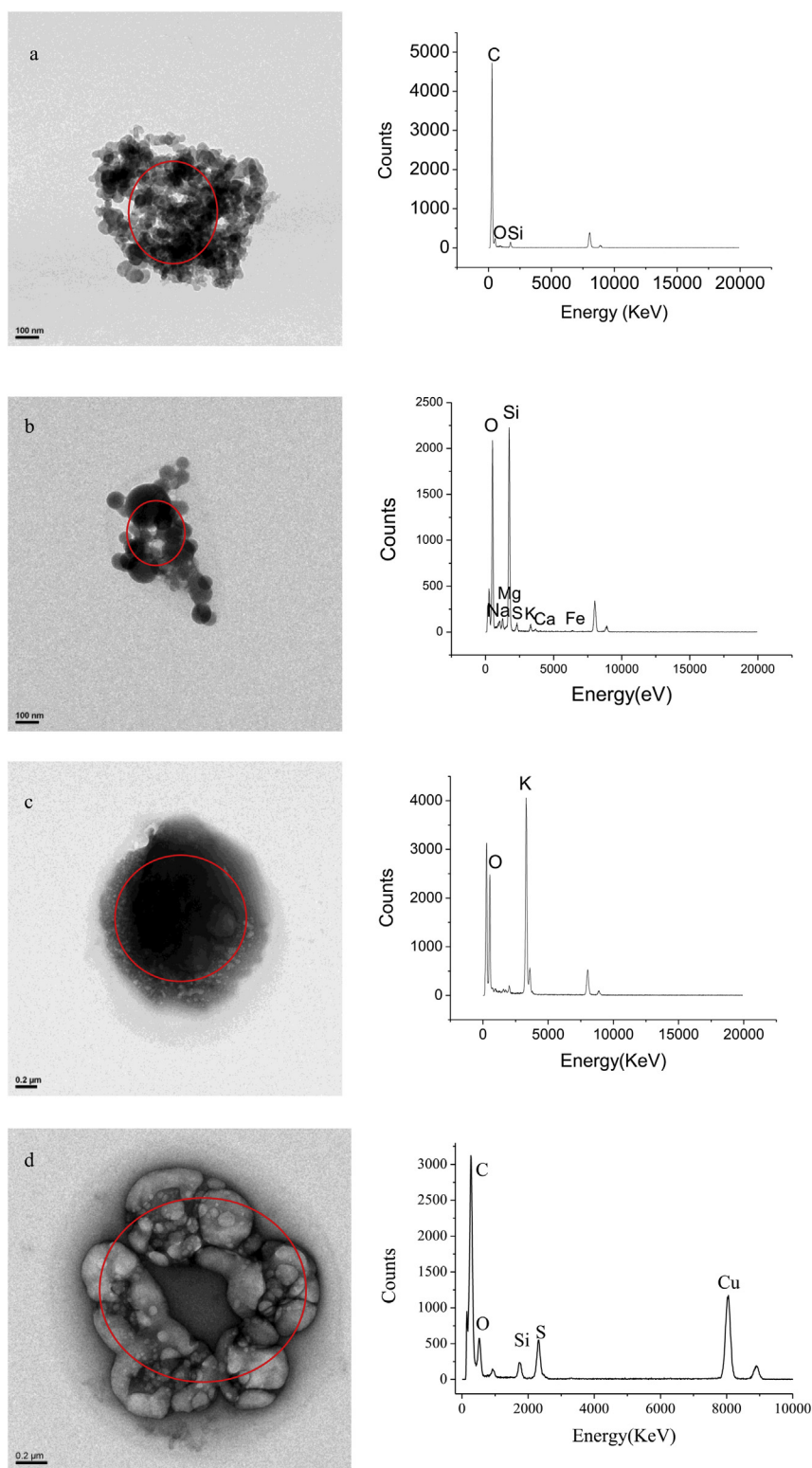


**Fig. 2.** TEM images of individual particles in the air of the Tibet Plateau. a: One complicated chain soot collected at the Shangri-La regional atmosphere background station. b: One aggregate of fly ash. EDX shows elemental composition of Si-rich fly ash. c: One K-rich particle, EDX shows composition of K-rich particle. d: One S-rich particle collected at Shangri-La. e: The same particle of Fig. 2d after EDX beam. f: One aggregate of mangy regular calcium sulfate rod. EDX shows elemental composition of  $\text{CaSO}_4$ . g: One mineral dust particle. h: Organic particle. i: One tar ball. j: One metal particle, EDX shows composition of Fe-rich particle.

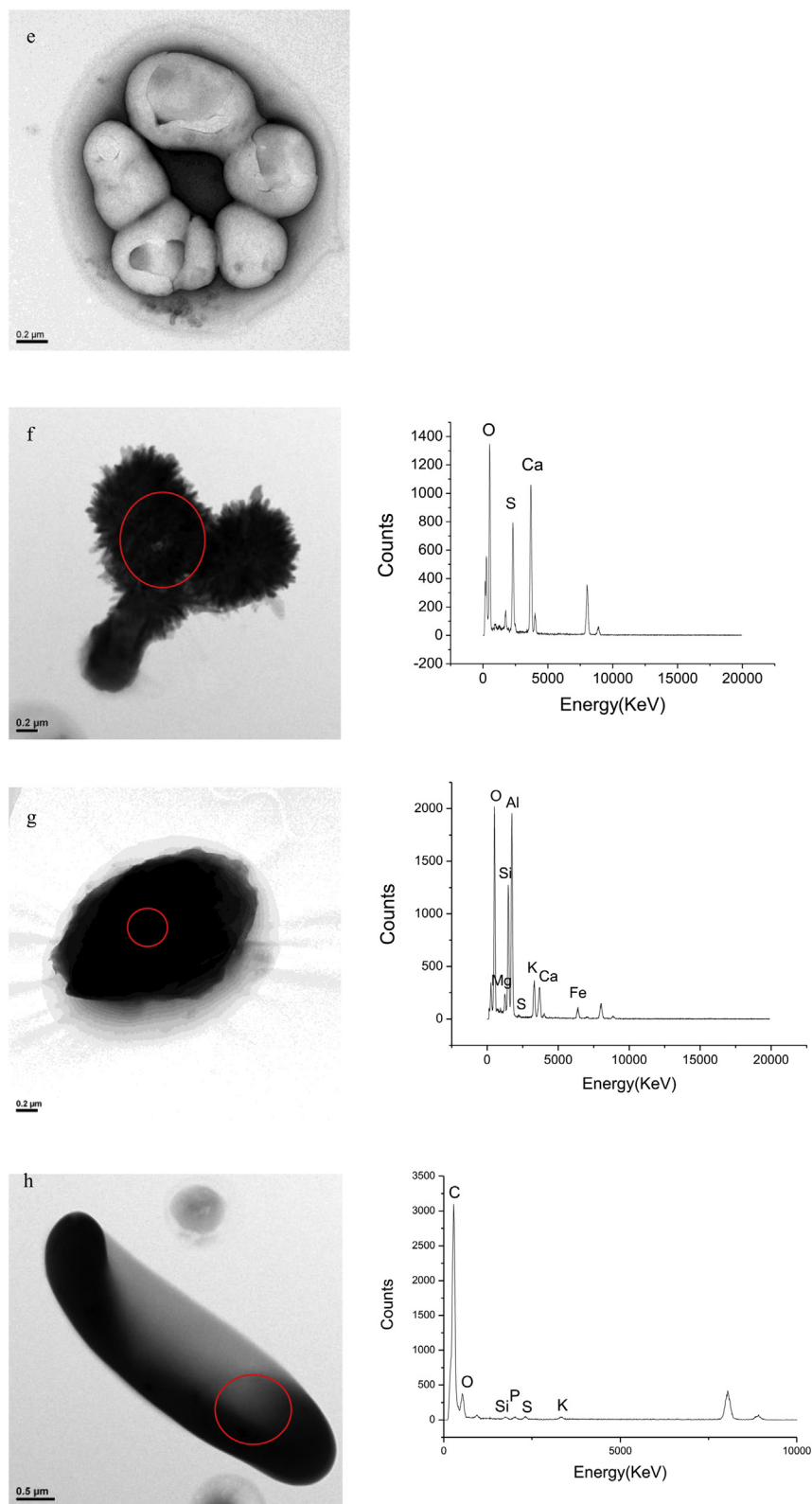


Fig. 2. (continued).



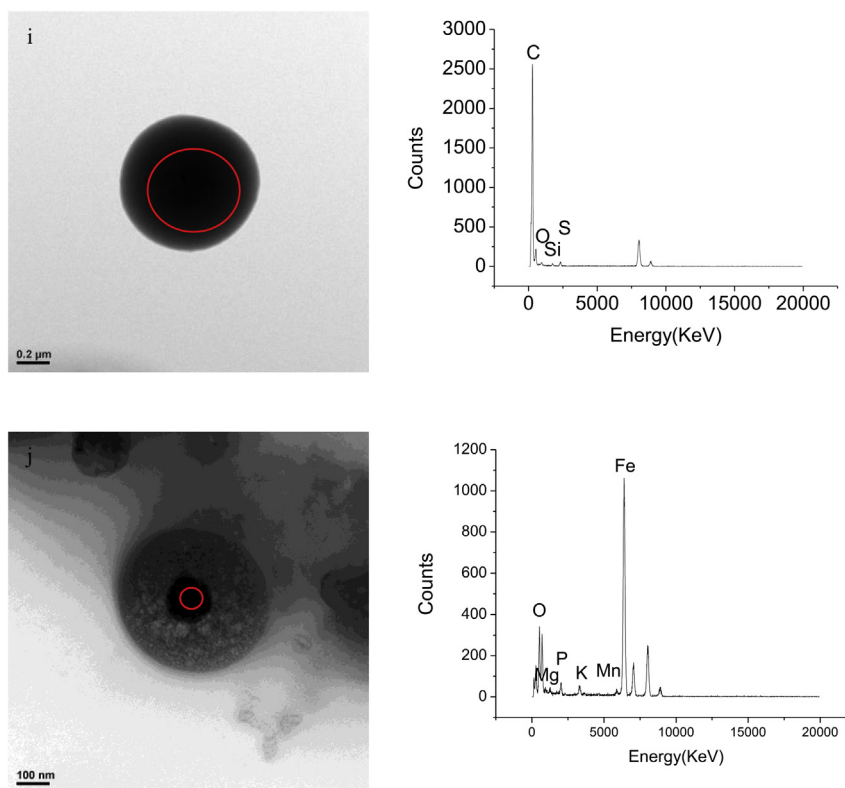


Fig. 2. (continued).

Metal particles at Shangri-La were mainly Fe- (Fig. 2j) and Zn-rich particles, with minor quantities of Mn- and Ti-rich particles. Spherical Fe-rich particle looks the same as fly ash in TEM image. Metal particles tend to be present in association with a visible coating formed through a secondary chemical reaction. Metal particles generally originate from industrial activities.

### 3.3. Relative abundance and size distribution of different aerosol particle types

In total, 397 particles were analyzed, and the proportions of different types of individual particles were counted. The results indicated that aerosol particles in Shangri-La consisted mainly of mineral particles (36.02%) and complex secondary particles (30.73%), followed by organic particles (17.38%), soot (8.06%), fly ash (6.08%), and metal particles (1.01%). The number-size distribution

of different types of particles (Fig. 3) demonstrated that the diameters of fly ash, soot, and metal particles were less than 2  $\mu\text{m}$ , and the contents (%) of fly ash and soot decreased with increasing particle size. Particles with diameters less than 2  $\mu\text{m}$  comprised 73% of the analyzed aerosol particles. By contrast, the content (%) of mineral particles increased increasing particle size; 84% of particles had diameters of 2–10  $\mu\text{m}$ .

## 4. Discussion

### 4.1. Mixing mechanisms of aerosol particles

According to the comprehensive analysis of the 292 analyzed aerosol particles, approximately 81% of the particles were internally or externally mixed with two or more aerosol components from different sources. These mixtures can be internally (multiple components within a particle) and externally (different components in different particles) mixed particles (Bauer and Koch, 2005). The components of externally mixed particles remain unchanged and can be easily judged from their appearance. Compositions and morphologies of internally mixed particles suggested that these particles were formed through condensation, dissolution, aqueous chemical reactions, and coagulation (Laskin et al., 2005; Nieminen et al., 2006; Zhang et al., 2005).

In Shangri-La, both relative fresh (Fig. 4a) and aged minerals were observed. However, most mineral particles were encapsulated by visible coatings (Fig. 4b and c) and thus were large. The coatings were composed of Ca, S, and sometimes N (inferred when no elements are detected in the coating), indicating that mineral particles were aged during atmospheric transport. Sullivan et al. (2007) indicated that the aging of Asian mineral dust particles occurred through heterogeneous chemical modifications by  $\text{HNO}_3$  and

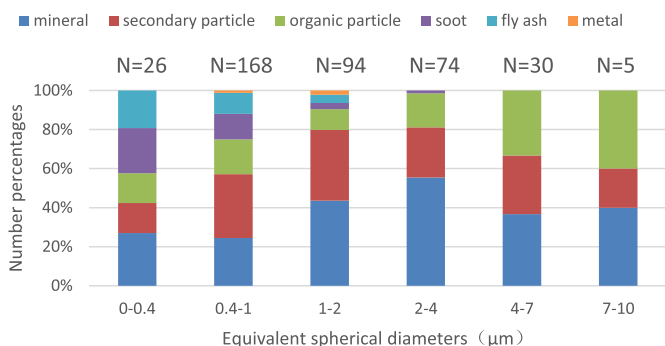


Fig. 3. Proportions of different individual aerosol particles in the air of the Shangri-La.

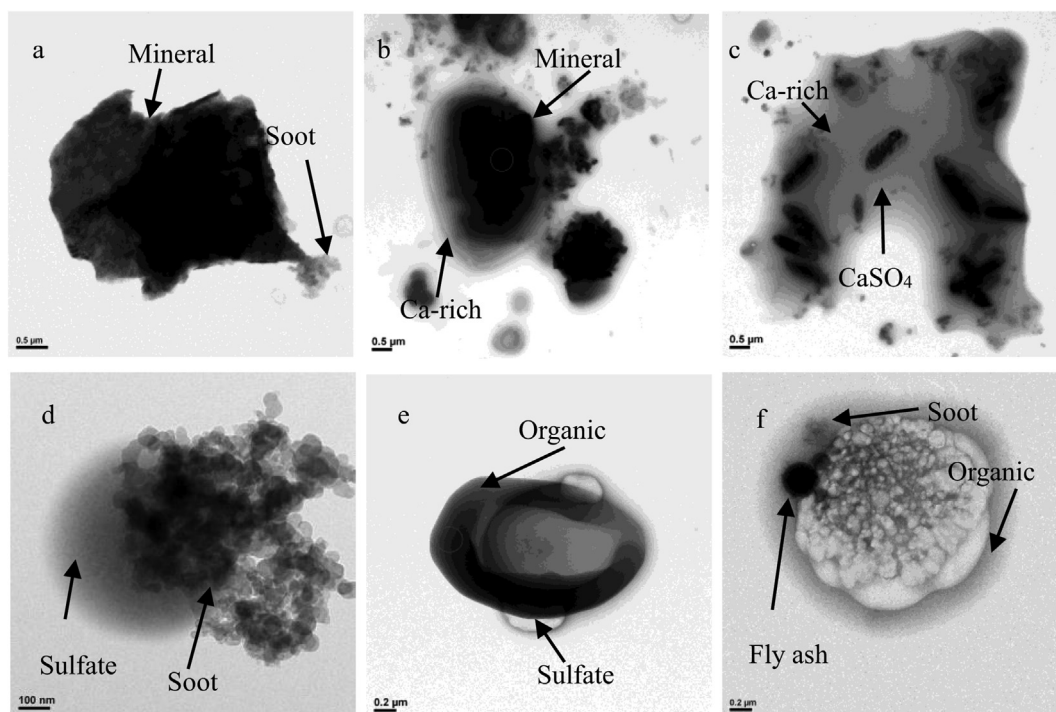


Fig. 4. TEM images of mixed individual aerosol particles in the air of the Tibet Plateau.

H<sub>2</sub>SO<sub>4</sub> and coagulation with (NH<sub>4</sub>)<sub>2</sub>SO<sub>4</sub>. Li and Shao (2009a) reported that mineral particles with visible coatings in haze contained N and S, and these particles probably underwent a few heterogeneous chemical modifications with HNO<sub>3</sub> and H<sub>2</sub>SO<sub>4</sub>. They demonstrated that these chemical reactions occurred on the surfaces of mineral dust particles containing calcite and dolomite components (Li and Shao, 2009b). Our results suggested that these visible coatings were probably formed through chemical reactions on the surface of the particles, possibly involving anthropogenic components, such as SO<sub>2</sub> and NO<sub>x</sub>.

Soot and organic materials from biomass burning were internally mixed with K- and S-rich particles (Fig. 4d and e). The rapid aging of fresh soot occurs in polluted urban air, particularly internally mixed with ammonium sulfate (Shi et al., 2008). Sulfate particles mainly act as a carrier for internally mixed particles, soot aggregates, and organic particles. Fine mineral particles mainly act as the nucleus of mixed particles (Fig. 4f). Thus, S-rich particles mixed with any fine insoluble aerosol particles (i.e., fly ash, soot, organic, mineral, and Fe-rich particles).

#### 4.2. Sources of aerosol particles

The formation of Ca-S particles, soot and K-rich particles, complex secondary particles, fly ash, metal particles, and mineral particles through atmospheric reactions, vehicle emissions, biomass burning, atmospheric reactions, coal combustion, industry emission, and crustal soil, respectively, has been reported elsewhere in China (Shi et al., 2003; Sun et al., 2006; Xie et al., 2008).

Back-trajectories are one of the simplest representations of the potential of emissions to travel from a source to a receptor (Beverland et al., 2000) and are widely used in tracing air mass transport (Suzuki et al., 2013). The 24-h isentropic backward trajectories in Shangri-La during the sampling period are depicted in

Fig. 5. Trajectories of air masses indicated that the air masses arriving at Shangri-La travelled through Northeast Burma, where a densely populated and industrialized setting favored fossil fuel burning. According to the element analysis and sulfuration state analysis results, most anthropogenic particles, such as metal particles, soot, and S-rich particles, were transported from Northeast Burma, a part of the Indian subcontinent.

#### 5. Conclusion

Detailed information on the morphologies, sizes, elemental compositions, and internal structures of individual aerosol particles at the Shangri-La regional atmosphere background station by TEM-EDX. More than 14 elements were detected in aerosol particles in Shangri-La. S were detected in more than 70% of the 292 analyzed particles. K in more than 50%, and Mg, Al, K, Ca, and Fe in approximately 30% of the 292 analyzed particles. Compared with the brown haze particles around Beijing, in which more than 18 elements were detected and S was present in more than 87% of the analyzed particles (Li and Shao, 2009a), the aerosol particles at Shangri-La were chemically less complex.

Aerosol particles in Shangri-La mainly contained mineral particles (36.02%) and complex secondary particles (30.73%), followed by organic particles (17.38%), soot (8.06%), fly ash (6.08%), and metal particles (1.01%). Fly ash, soot, and metal particles were less than 2 μm in diameter. The particles with diameters less than 2 μm comprised 73% of the analyzed aerosol particles.

The visible coatings of the mineral particles were probably formed through chemical reactions on the particle surfaces, and S-rich particles were mixed with fine insoluble aerosol particles (i.e., fly ash, soot, organic, mineral, and Fe-rich particles).

The air masses arriving at Shangri-La travelled through Northeast Burma, where a densely populated and industrialized setting favored fossil fuel burning and coal combustion.

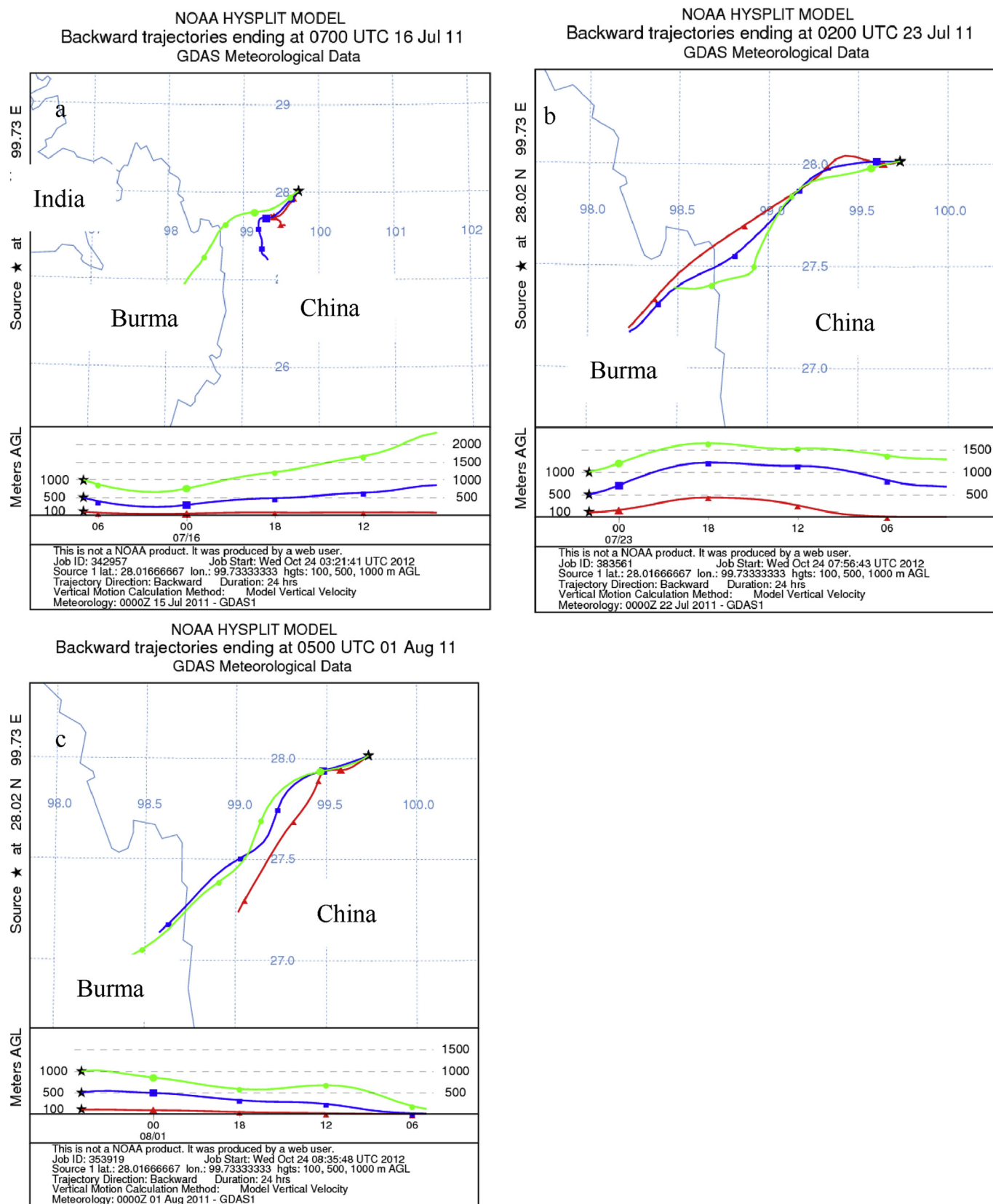


**Fig. 5.** 24-h air mass back trajectories arriving to Shangri-La. (a), (b) and (c) are on 16th July (the first sampling day), 23rd July (the middle of the sampling period) and 1st August 2011 (the last day of sampling), respectively. Solid dots on each line represent 6-h intervals.



## Acknowledgements

Financial support was provided by the Public Welfare (meteorological) Project (NO.GYHY201106023) and Projects of International Cooperation and Exchanges of the National Natural Science Foundation of China (Grant No. 41571130031).

## References

- Adachi, K., Buseck, P.R., 2008. Internally mixed soot, sulfates, and organic matter in aerosol particles from Mexico City. *Atmos. Chem. Phys.* 8 (21), 6469–6481.
- Adachi, K., Buseck, P.R., 2010. Hosted and free-floating metal-bearing atmospheric nanoparticles in Mexico City. *Environ. Sci. Technol.* 44 (7), 2299–2304.
- Adachi, K., Zaizen, Y., Kajino, M., Igarashi, Y., 2014. Mixing state of regionally transported soot particles and the coating effect on their size and shape at a mountain site in Japan. *J. Geophys. Res. Atmos.* 119 (9), 5386–5396.
- Bauer, S.E., Koch, D., 2005. Impact of heterogeneous sulfate formation at mineral dust surfaces on aerosol loads and radiative forcing in the Goddard Institute for Space Studies general circulation model. *J. Geophys. Res. Atmos.* 110 (D17), 1984–2012.
- Beverland, I.J., Tunes, T., Sozanska, M., Elton, R.A., Agius, R.M., Heal, M.R., 2000. Effect of long-range transport on local PM<sub>10</sub> concentrations in the UK. *Int. J. Environ. Heal. R* 10 (3), 229–238.
- Braziewicz, J., Kownacka, L., Majewska, U., Korman, A., 2004. Elemental concentrations in tropospheric and lower stratospheric air in a Northeastern region of Poland. *Atmos. Environ.* 38 (13), 1989–1996.
- Buseck, P.R., Jacob, D.J., Pósfai, M., Li, J., Anderson, J.R., 2000. Minerals in the air: an environmental perspective. *Int. Geol. Rev.* 42 (7), 577–593.
- Chakrabarty, R.K., Moosmüller, H., Garro, M.A., Arnott, W.P., Walker, J., Susott, R.A., Babbitt, R.E., Wold, C.E., Lincoln, E.N., Hao, W.M., 2006. Emissions from the laboratory combustion of wildland fuels: particle morphology and size. *J. Geophys. Res. Atmos.* 111 (D7), 1984–2012.
- Cong, Z., Kang, S., Zhang, Y., Li, X., 2010a. Atmospheric wet deposition of trace elements to central Tibetan Plateau. *Appl. Geochem.* 25 (9), 1415–1421.
- Cong, Z., Kang, S., Dong, S., Liu, X., Qin, D., 2010b. Elemental and individual particle analysis of atmospheric aerosols from high Himalayas. *Environ. Monit. Assess.* 160 (1–4), 323–335.
- Duo, B., Zhang, Y., Kong, L., Fu, H., Hu, Y., Chen, J., Li, L., Qiong, A., 2015. Individual particle analysis of aerosols collected at Lhasa city in the Tibetan plateau. *J. Environ. Sci.* 29, 165–177.
- Fang, S., Li, Z., Zhou, L., Xu, L., 2012. Variation of CH<sub>4</sub> concentrations at Yunnan Xianggelila background station in China. *Acta. Sci. Circumst.* 32 (10), 2568–2574.
- Fattori, I., Becagli, S., Bellandi, S., Castellano, E., Innocenti, M., Mannini, A., Severi, M., Vitale, V., Udisti, R., 2005. Chemical composition and physical features of summer aerosol at Terra Nova Bay and Dome C, Antarctica. *J. Environ. Monit.* 7 (12), 1265–1274.
- Fu, H., Zhang, M., Li, W., Chen, J., Wang, L., Quan, X., Wang, W., 2012. Morphology, composition and mixing state of individual carbonaceous aerosol in urban Shanghai. *Atmos. Chem. Phys.* 12 (2), 693–707.
- Gao, C., Yang, H., Zhou, H., 2013. An analysis of air pollution characteristics and its development trend in urban center of Shangri-La. *Environ. Sci. Surv.* 32 (1), 49–50.
- Griessbach, S., Hoffmann, L., Höpfner, M., Riese, M., Spang, R., 2013. Scattering in infrared radiative transfer: a comparison between the spectrally averaging model JURASSIC and the line-by-line model KOPRA. *J. Quant. Spectrosc. Radiat.* 127, 102–118.
- Guo, Z., Li, Z., Farquhar, J., Kaufman, A.J., Wu, N., Li, C., Dickerson, R.R., Wang, P., 2010. Identification of sources and formation processes of atmospheric sulfate by sulfur isotope and scanning electron microscope measurements. *J. Geophys. Res. Atmos.* 115 (D7), 1984–2012.
- Hu, Y., Shao, L., Wang, J., Fan, J., Hou, C., 2013. Types and size distribution of individual particles in the Tibetan Plateau. *Acta Petrologica Mineralogica* 32 (6), 863–872.
- Huang, J., Kang, S., Shen, C., Cong, Z., Liu, K., Wang, W., Liu, L., 2010. Seasonal variations and sources of ambient fossil and biogenic-derived carbonaceous aerosols based on <sup>14</sup>C measurements in Lhasa, Tibet. *Atmos. Res.* 96 (4), 553–559.
- Laskin, A., Iedema, M.J., Ichkovich, A., Graber, E.R., Taraniuk, I., Rudich, Y., 2005. Direct observation of completely processed calcium carbonate dust particles. *Faraday Discuss.* 130, 453–468.
- Li, W., Shao, L., 2009a. Transmission electron microscopy study of aerosol particles from the brown hazes in northern China. *J. Geophys. Res. Atmos.* 114 (D9), 1984–2012.
- Li, W.J., Shao, L.Y., 2009b. Observation of nitrate coatings on atmospheric mineral dust particles. *Atmos. Chem. Phys.* 9 (6), 1863–1871.
- Li, W., Shao, L., Wang, Z., Shen, R., Yang, S., Tang, U., 2010a. Size, composition, and mixing state of individual aerosol particles in a South China coastal city. *J. Environ. Sci.* 22 (4), 561–569.
- Li, W.J., Shao, L.Y., Buseck, P.R., 2010b. Haze types in Beijing and the influence of agricultural biomass burning. *Atmos. Chem. Phys.* 10 (17), 8119–8130.
- Li, W.J., Zhang, D.Z., Shao, L.Y., Zhou, S.Z., Wang, W.X., 2011. Individual particle analysis of aerosols collected under haze and non-haze conditions at a high-elevation mountain site in the North China plain. *Atmos. Chem. Phys.* 11 (22), 11733–11744.
- Li, W., Shi, Z., Yan, C., Yang, L., Dong, C., Wang, W., 2013. Individual metal-bearing particles in a regional haze caused by firecracker and firework emissions. *Sci. Total. Environ.* 443, 464–469.
- Li, W.J., Chen, S.R., Xu, Y.S., Guo, X.C., Sun, Y.L., Yang, X.Y., Wang, Z.F., Zhao, X.D., Chen, J.M., Wang, W.X., 2015. Mixing state and sources of submicron regional background aerosols in the northern Qinghai-Tibetan Plateau and the influence of biomass burning. *Atmos. Chem. Phys.* 15, 13365–13376.
- Li, W., Shao, L., Zhang, D., Ro, C.U., Hu, M., Bi, X., Geng, H., Matsuki, A., Niu, H., Chen, J., 2016. A review of single aerosol particle studies in the atmosphere of East Asia: morphology, mixing state, source, and heterogeneous reactions. *J. Clean. Prod.* 112, 1330–1349.
- Lin, W., Xu, X., Yu, D., Dai, X., Zhang, Z., 2009. Quality control for reactive gases observation at Longfengshan regional atmospheric background monitoring station. *Meteorol. Mon.* 35, 93–100.
- Lu, S., Shao, L., Wu, M., Zheng, J., Chen, X., 2007. Chemical elements and their source apportionment of PM<sub>10</sub> in Beijing urban atmosphere. *Environ. Monit. Assess.* 133 (1–3), 79–85.
- Ma, J., Lin, W., Zheng, X., Xu, X., Li, Z., Yang, L., 2014. Influence of air mass downward transport on the variability of surface ozone at Xianggelila Regional Atmosphere Background Station, southwest China. *Atmos. Chem. Phys.* 14 (11), 5311–5325.
- Marple, V.A., Rubow, K.L., Olson, B.A., 1993. Inertial, gravitational, centrifugal, and thermal collection techniques. In: Willike, K., Baron, P.A. (Eds.), *Aerosol Measurement*. Van Nostrand Reinhold, New York, pp. 206–233.
- Ming, J., Xiao, C., Sun, J., Kang, S., Bonasoni, P., 2010. Carbonaceous particles in the atmosphere and precipitation of the Nam Co region, central Tibet. *J. Environ. Sci.* 22 (11), 1748–1756.
- Moffet, R.C., Prather, K.A., 2009. In-situ measurements of the mixing state and optical properties of soot with implications for radiative forcing estimates. *P. Natl. Acad. Sci.* 106 (29), 11872–11877.
- Nieminen, J.V., Saarikoski, S., Tervahattu, H., Mäkelä, T., Hillamo, R., Vehkamäki, H., Sogacheva, L., Kulmala, M., 2006. Changes in background aerosol composition in Finland during polluted and clean periods studied by TEM/EDX individual particle analysis. *Atmos. Chem. Phys.* 6 (12), 5049–5066.
- Pósfai, M., Gelencsér, A., Simonics, R., Arató, K., Li, J., Hobbs, P.V., Buseck, P.R., 2004. Atmospheric tar balls: particles from biomass and biofuel burning. *J. Geophys. Res. Atmos.* 109 (D6), 1984–2012.
- Pósfai, M., Buseck, P.R., 2010. Nature and climate effects of individual tropospheric aerosol particles. *Annu. Rev. Earth. Pl. Sc.* 38, 17–43.
- Pósfai, M., Axisa, D., Tompa, É., Freney, E., Bruinjes, R., Buseck, P.R., 2013. Interactions of mineral dust with pollution and clouds: an individual-particle TEM study of atmospheric aerosol from Saudi Arabia. *Atmos. Res.* 122, 347–361.
- Qiu, J., 2008. China: the third pole. *Nature* 454, 393–396.
- Rozanov, V.V., Rozanov, A.V., Kokhanovsky, A.A., Burrows, J.P., 2014. Radiative transfer through terrestrial atmosphere and ocean: software package SCIA-TRAN. *J. Quant. Spectrosc. Radiat.* 133, 13–71.
- Shao, L., Li, J., Zhao, H., Yang, S., Li, H., Li, W., Jones, T., Sexton, K., Bérubé, K., 2007. Associations between particle physicochemical characteristics and oxidative capacity: an indoor PM<sub>10</sub> study in Beijing, China. *Atmos. Environ.* 41 (26), 5316–5326.
- Shi, Y., Ge, M., Wang, W., 2012. Hygroscopicity of internally mixed aerosol particles containing benzoic acid and inorganic salts. *Atmos. Environ.* 60, 9–17.
- Shi, Z., Shao, L., Jones, T.P., Whittaker, A.G., Lu, S., Berube, K.A., He, T., Richards, R.J., 2003. Characterization of airborne individual particles collected in an urban area, a satellite city and a clean air area in Beijing, 2001. *Atmos. Environ.* 37 (29), 4097–4108.
- Shi, Z., Zhang, D., Ji, H., Hasegawa, S., Hayashi, M., 2008. Modification of soot by volatile species in an urban atmosphere. *Sci. Total. Environ.* 389 (1), 195–201.
- Smith, S., Ward, M., Lin, R., Brydson, R., Dall'Osto, M., Harrison, R.M., 2012. Comparative study of single particle characterisation by transmission electron microscopy and time-of-flight aerosol mass spectrometry in the London atmosphere. *Atmos. Environ.* 62, 400–407.
- Sullivan, R.C., Guazzotti, S.A., Sodeman, D.A., Prather, K.A., 2007. Direct observations of the atmospheric processing of Asian mineral dust. *Atmos. Chem. Phys.* 7 (5), 1213–1236.
- Sun, Y., Zhuang, G., Tang, A., Wang, Y., An, Z., 2006. Chemical characteristics of PM<sub>2.5</sub> and PM<sub>10</sub> in haze-fog episodes in Beijing. *Environ. Sci. Technol.* 40 (10), 3148–3155.
- Suzuki, K., Yamanouchi, T., Kawamura, K., Motoyama, H., 2013. The spatial and seasonal distributions of air-transport origins to the Antarctic based on 5-day backward trajectory analysis. *Polar Sci.* 7 (3), 205–213.
- Thompson, J.E., Hayes, P.L., Jimenez, J.L., Adachi, K., Zhang, X., Liu, J., Weber, R.J., Buseck, P.R., 2012. Aerosol optical properties at Pasadena, CA during CalNex 2010. *Atmos. Environ.* 55, 190–200.
- Tivanski, A.V., Hopkins, R.J., Tylliszczak, T., Gilles, M.K., 2007. Oxygenated interface on biomass burn tar balls determined by single particle scanning transmission X-ray microscopy. *J. Phys. Chem. A* 111 (25), 5448–5458.
- Toscano, G., Gambaro, A., Moret, I., Capodaglio, G., Turetta, C., Cescon, P., 2005. Trace metals in aerosol at Terra Nova bay, Antarctica. *J. Environ. Monit.* 7 (12), 1275–1280.

- Ueda, S., Hirose, Y., Miura, K., Okochi, H., 2014. Individual aerosol particles in and below clouds along a Mt. Fuji slope: modification of sea-salt-containing particles by in-cloud processing. *Atmos. Res.* 137, 216–227.
- Vester, B.P., Ebert, M., Barnert, E.B., Schneider, J., Kandler, K., Schütz, L., Weinbruch, S., 2007. Composition and mixing state of the urban background aerosol in the Rhein-Main area (Germany). *Atmos. Environ.* 41 (29), 6102–6115.
- Wan, X., Kang, S., Wang, Y., Xin, J., Liu, B., Guo, Y., Wen, T., Zhuang, G., Cong, Z., 2015. Size distribution of carbonaceous aerosols at a high-altitude site on the central Tibetan Plateau (Nam Co Station, 4730m asl). *Atmos. Res.* 153, 155–164.
- Wang, J., Cubison, M.J., Aiken, A.C., Jimenez, J.L., Collins, D.R., 2010. The importance of aerosol mixing state and size-resolved composition on CCN concentration and the variation of the importance with atmospheric aging of aerosols. *Atmos. Chem. Phys.* 10 (15), 7267–7283.
- Xie, M., Zhang, W., 2000. *Climate Prediction Method and Model in Short-term in Yunnan*. China Meteorological Press, Beijing.
- Xie, S.D., Liu, Z., Chen, T., Hua, L., 2008. Spatiotemporal variations of ambient PM<sub>10</sub> source contributions in Beijing in 2004 using positive matrix factorization. *Atmos. Chem. Phys.* 8 (10), 2701–2716.
- Yang, F., Chen, H., Du, J., Yang, X., Gao, S., Chen, J., Geng, F., 2012. Evolution of the mixing state of fine aerosols during haze events in Shanghai. *Atmos. Res.* 104, 193–201.
- Yang, L., 2013. Variation of visibility at Yunnan Xianggelila background station in China. *J. Green Sci. Technol.* 10, 29–31.
- Yao, X., Lau, A.P., Fang, M., Chan, C.K., Hu, M., 2003. Size distributions and formation of ionic species in atmospheric particulate pollutants in Beijing, China: 1-inorganic ions. *Atmos. Environ.* 37 (21), 2991–3000.
- Zhang, D., Iwasaka, Y., Shi, G., 2001. Soot particles and their impacts on the mass cycle in the Tibetan atmosphere. *Atmos. Environ.* 35 (34), 5883–5894.
- Zhang, D., Iwasaka, Y., Shi, G., Zang, J., Hu, M., Li, C., 2005. Separated status of the natural dust plume and polluted air masses in an Asian dust storm event at coastal areas of China. *J. Geophys. Res. Atmos.* 110 (D6), 1984–2012.
- Zhang, G., Bi, X., Li, L., Chan, L.Y., Li, M., Wang, X., Sheng, G., Fu, J., Zhou, Z., 2013. Mixing state of individual submicron carbon-containing particles during spring and fall seasons in urban Guangzhou, China: a case study. *Atmos. Chem. Phys.* 13 (9), 4723–4735.
- Zhao, S., Ming, J., Sun, J., Xiao, C., 2013. Observation of carbonaceous aerosols during 2006–2009 in Nyainqentanglha Mountains and the implications for glaciers. *Environ. Sci. Pollut. R.* 20 (8), 5827–5838.